

Calorimetric Studies of PP/Mater-Bi Blends Aged in Soil

Ana Cadenato,¹ Xavier Ramis,¹ Josep Ma Salla,¹ Josep Ma Morancho,¹ L. Contat-Rodrigo,²
A. Vallés-Lluch,² A. Ribes-Greus²

¹Laboratory of Thermodynamics, Escola Tècnica Superior d'Enginyeria Industrial Barcelona, Universidad Politècnica de Catalunya, Avenida Diagonal 647, 08028 Barcelona, Spain

²Department of Applied Thermodynamics, Escuela Técnica Superior de Ingenieros Industriales de Valencia, Apartado 22012, 46071 Valencia, Spain

Received 1 May 2004; accepted 6 February 2005

DOI 10.1002/app.22084

Published online in Wiley InterScience (www.interscience.wiley.com).

ABSTRACT: Blends of polypropylene and a commercial biodegradable additive (Mater-Bi AF05H) were subjected to a soil burial test for 1 year. The effect of the degradation process on the morphology of the blend was studied by differential scanning calorimetry. The melting and crystallization temperatures, degree of crystallinity, lamellar thickness distribution, and crystallization kinetics were analyzed

for both the nondegraded and degraded blends and for the pure components before blending and degradation. © 2006 Wiley Periodicals, Inc. *J Appl Polym Sci* 100: 3446–3453, 2006

Key words: additives; biodegradable; degradation; differential scanning calorimetry (DSC); poly(propylene) (PP)

INTRODUCTION

Polypropylene (PP) is a synthetic polymer that has been designed and produced to resist very well biotic environmental degradation. However, in most of its applications, this material is rejected after a short period of use. This has led to an important increase in the volume of the waste of this plastic for a long time.

A solution to this problem could be the incorporation of biodegradable biopolymers into the polyolefinic matrix.¹ Biodegradable materials constitute a family of polymers that are easily degraded by living organisms. Under the Mater-Bi trademark, a new generation of biodegradable plastic-like materials based on starch and different synthetic components can be found in the market. In this study, Class A Mater-Bi, made of starch and ethylene vinyl-alcohol (EVOH) copolymers, was mixed with PP.²

The degradation process is understood as the result of irreversible changes in the physical properties of polymers, caused by chemical reactions involving bond scission in the backbones of macromolecules.³ The degradation mechanism in soil of the blends of PP and biodegradable materials is a complex process.^{4–6}

The enzymatic hydrolysis of biopolymers under biotic conditions reduces the mechanical integrity of the polyolefinic matrix, leading to its easy deterioration and maybe even promoting its subsequent degradation.

There is a wide variety of conventional analytical techniques that provide information about the microstructural modifications that are thought to originate from polymer degradation. However, there is also a well-established set of analytical techniques, including thermal analysis (and in particular calorimetry), that are closely related to the macroscopic properties of polymers.

Calorimetric methods are based on the measurement of the intrinsic change in the absorption or emission of heat by the polymer as it undergoes a transformation or reaction. When heating is performed under strictly controlled conditions, qualitative and quantitative information about the effects of degradation on the structure and other important properties of the degraded material can be obtained. From the analysis of both the calorimetric thermograms and the crystallization kinetics, the effect of degradation on the polymer morphology can be determined.

In this study, the morphological changes of a PP/Mater-Bi blend during degradation in soil were analyzed by differential scanning calorimetry (DSC).

EXPERIMENTAL

Material preparation

PP 1148-TC, supplied by BASF (Rudolfstadt, Germany), was blended with Mater-Bi AF05H supplied

Correspondence to: A. Ribes-Greus (aribes@ter.upv.es).

Contract grant sponsor: CICYT; contract grant number: MAT2000-1002-C02-02.

Contract grant sponsors: Comisión Interministerial de Ciencia Y Tecnología and Fondos Europeos de Desarrollo Regional; contract grant numbers: PPQ2001-2764-C03-02 and PPQ2001-2764-C03-01.

by Novamont North America (Ridgefield, CT). Mater-Bi AF05H is a starch-based additive that contains thermoplastic starch highly complexed with EVOH copolymers, with a starch content close to 50 wt %.

A homogeneous mixture with 50/50 wt % of PP/Mater-Bi AF05H was initially prepared from the melt in a Brabender Plasticorder PL 2100 rheometer (Duisburg, Germany). The blend was then cut as nut coal and compression-molded into rectangular bars (68 × 12 × 1.8 mm) with an M Carver press (Wabash, IN).

Samples of pure PP and Mater-Bi AF05H were also compression-molded from pellets to be used as control materials. Both pure and blended samples were taken apart to compare with the samples degraded in soil.

Soil burial test

The soil burial test was carried out according to the DIN 53739 International Norm⁷ for a period of 1 year. Samples were buried in biologically active soil contained in rectangular plastic boxes, which were kept opened to ensure a continuous supply of fresh oxygen.⁸ The soil used was a 50/50 wt % mixture of a soil extract picked up from a culture field and a soil typically used in tree nurseries for pine growth. The test was carried out in a Hereaus B12 culture oven at a constant temperature of $28 \pm 0.5^\circ\text{C}$, with periodical control of the pH and the water content of the soil. The pH was maintained at approximately 7.3 ± 0.1 (measured in water), and the humidity was maintained at $65.0 \pm 0.5\%$.

Samples were removed after different periods of time: 20 days and 4, 6, 8, 10, and 12 months. Pure samples were only removed at the end of the test. After removal, all of the samples were carefully washed with a soap solution to stop the degradation process and were blotted before analysis.

DSC measurements

DSC measurements were performed on a Mettler-Toledo DSC-30 instrument (Greifensee, Switzerland), previously calibrated with an indium standard, under a nitrogen atmosphere. About 10 mg of sample was accurately weighed in a standard aluminum pan. The pans were sealed and pierced. Dynamic and isothermal measurements were carried out.

Dynamic measurements

All samples were submitted to the same process. Samples were initially heated from 25 to 200°C at a rate of $10^\circ\text{C}/\text{min}$ (first scan). Then, they were kept at 200°C for 5 min to ensure that the sample had melted and that its thermal history was erased. Samples were then cooled from 200 to 25°C at a rate of $10^\circ\text{C}/\text{min}$, and

their crystallization processes were analyzed. Finally, samples were heated again from 25 to 200°C at a rate of $10^\circ\text{C}/\text{min}$ (second scan). Measurements were repeated to ensure errors of $\pm 0.01^\circ\text{C}$ for melting temperatures (T_m 's) and ± 0.05 for crystalline contents (χ).

Isothermal measurements

To study isothermal crystallization, the samples were also submitted to the following process. Samples were initially heated from 25 to 200°C at a rate of $10^\circ\text{C}/\text{min}$. The temperature was then kept at 200°C for 5 min. Samples were then cooled at a rate of $80^\circ\text{C}/\text{min}$ from 200°C to the crystallization temperature (T_c ; 136, 138, 140, 142, and 144°C). After their crystallization, samples were cooled again to 120°C at a rate of $80^\circ\text{C}/\text{min}$. Finally, samples were heated from 120 to 200°C at a rate of $10^\circ\text{C}/\text{min}$.

Fourier transform infrared spectroscopy (FTIR)

A FTIR Bomem Michelson MB100 spectrophotometer (Quebec, Canada) with a resolution of 4 cm^{-1} in the absorbance mode was used to determine FTIR spectra in the range $400\text{--}4000\text{ cm}^{-1}$. Samples were placed in an attenuated total reflection accessory with thermal control and a diamond crystal (Golden Gate Heated Single Reflection Diamond ATR, Specac-Teknokroma, Kent, UK).

RESULTS AND DISCUSSION

Calorimetric analysis was used to study T_m , the crystalline content, and the lamellar thickness (l) distribution during the degradation process. The kinetic parameters of the crystallization of the degraded samples were also calculated.

Figure 1 shows the DSC thermograms of the undegraded PP, Mater-Bi, and their blend.

The T_m 's of all the samples were directly determined from the thermograms (Table I). The T_m corresponded to the value of the maximum of each endothermic peak.

The first scan of pure PP showed its typical DSC thermogram, which consisted on a main endotherm with maximum around 168°C .

The first scan of pure Mater-Bi displayed two endothermic peaks around 133 and 156°C . This suggested that EVOH and starch, the main components of Mater-Bi, formed an heterogeneous mixture. Sousa et al.⁹ associated the low temperature peak to the crystalline phase of starch and the high temperature peak to the crystalline phase of EVOH.

The PP/Mater-Bi blends exhibited three endotherms, which could be assigned to those of PP and Mater-Bi. A shift of all the endotherms was observed

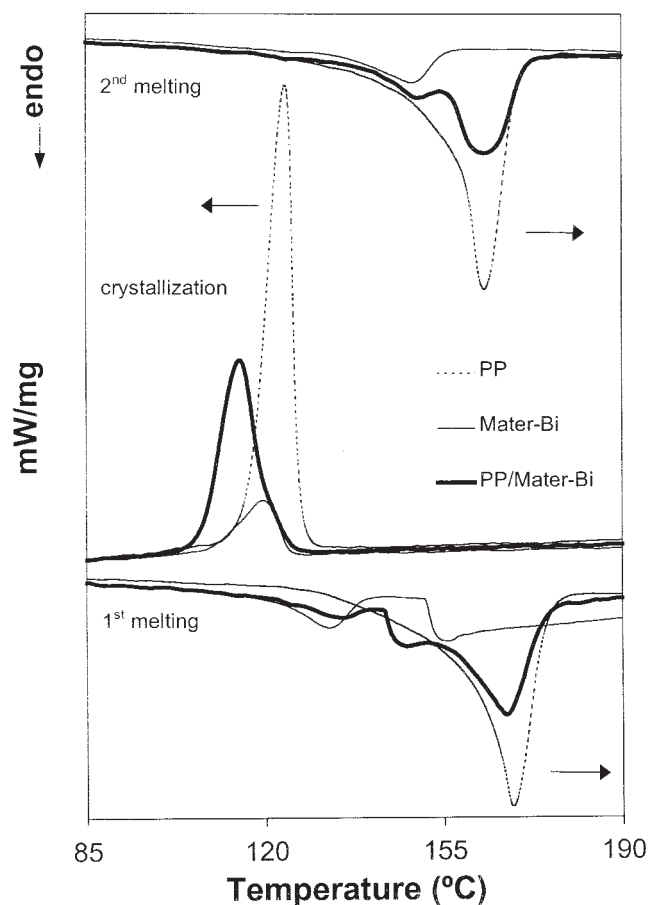


Figure 1 DSC thermograms of the first melting, crystallization, and second melting of the PP/Mater-Bi blend and the pure components.

when PP and Mater-Bi were mixed, indicating a certain interaction of both components.

The melt enthalpy is the difference between the enthalpy of the melt state (H_a) and the enthalpy of the crystalline state (H_c). The crystalline content (χ) of the control samples was calculated according to the equation $\chi = (H_a - H_c)/H_m$. The difference between H_a and

H_c was directly obtained from the thermogram. H_m is the change in the melting enthalpy of a perfect crystal of infinite size. These values were estimated as proposed by Van Krevelen¹⁰ from additive group contributions. The obtained values were 207.2 J/g for PP and 168.2 J/g for Mater-Bi. All the results are listed in Table I.

In the first melting scan, PP and the PP/Mater-Bi blend had similar crystallinities. However, in the second melting scan (after crystallization), the melt of the starch was not observed (Fig. 1). As a result, the crystallinity of Mater-Bi decreased, and the blend exhibited a lower crystallinity than PP.

Figures 2–4 show the thermograms of the PP/Mater-Bi blends as a function of the degradation time in soil. Table II summarizes the calorimetric parameters of these thermograms.

For these samples, the maximum lamellar thickness (l_{\max}) of PP was also calculated from its T_m according to the procedure proposed by Wlochowicz and Eder,¹¹ with the Thomson equation for l :

$$T_m = T_m^0 \left[1 - \left(\frac{2\sigma_e}{\Delta h_m l} \right) \right] \quad (1)$$

with the following parameters for PP:¹¹ equilibrium melting temperature of an infinite crystal (T_m^0) = 457 K, enthalpy of fusion per unit volume (Δh_m) = $1.34 \cdot 10^8$ J/m³, and surface free energy of the basal plane = $49.6 \cdot 10^{-3}$ J/m².

After studying the first melting process, we concluded that the peak temperature increased until the fourth degradation month and then remained almost constant around a lower value. The same tendency was observed for the maximum of the l distribution of PP. These results agreed with the increase of crystallinity until the fourth month, as calculated from the first melting. Hawkins¹² suggested that the crystalline content in a semicrystalline polymer is determined by the amorphous phase, which restricts the crystalliza-

TABLE I
Calorimetric Parameters of the Undegraded Materials

Process	Material	T_m (°C)		Δh_m (J/g)	χ (%)
		Main peak	Secondary peak		
First melting	PP	168.5	—	107.7	52.0
	Mater-Bi	156.3	133.2	71.6	42.6
	PP/Mater-Bi	167.3	134.6 148.0	99	52.8
Crystallization	PP	123.7	—	102.6	49.5
	Mater-Bi	119.8	—	20.6	12.2
	PP/Mater-Bi	115.6	—	64	34.1
Second melting	PP	163.4	—	103.7	50.0
	Mater-Bi	149.0	—	20.9	12.4
	PP/Mater-Bi	163.3	150.2	70	37.3

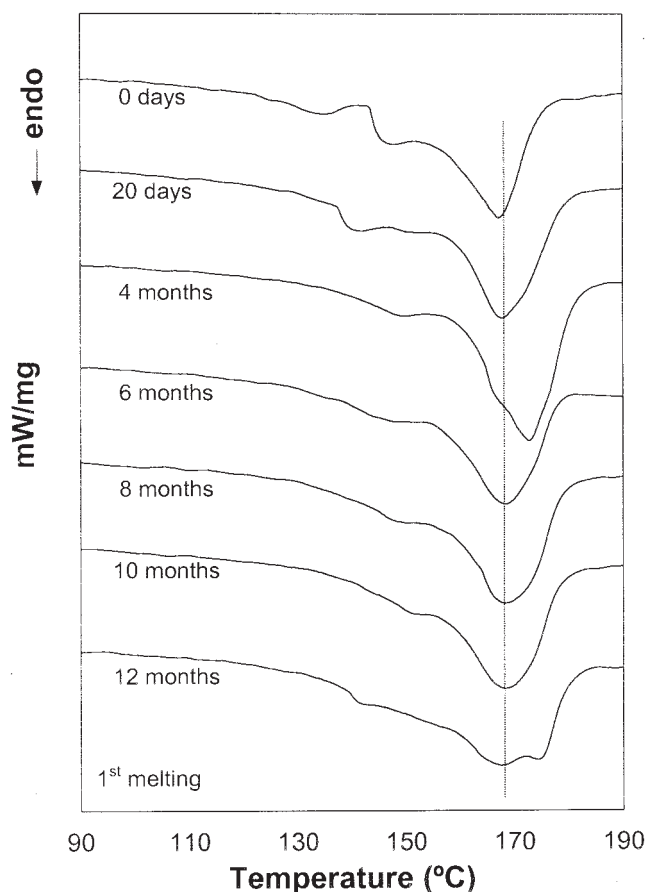


Figure 2 First melting of the PP/Mater-Bi blend as a function of the exposure time in soil.

tion process. As chain scissions in the amorphous phase can encourage the crystallization process, an increase in the crystalline content of a semicrystalline polymer must be considered as a degradation sign. For the blend under study, this material underwent a certain degradation until the fourth month, and then, its degradation process seemed to slow down.

In the first melting scan, the l distribution got wider, and the calorimetric signal became more complicated with degradation time. It seemed that the material became more crystalline and less homogeneous as the degradation time increased. This last effect disappeared after the thermal history of the material was deleted, and it was not observed in the second melting scan, where all of the thermograms exhibited similar l distributions. Because in semicrystalline polymers degradation starts in the amorphous phase and the interfacial regions, such changes observed at the first melting could then be related to a change in the morphological regions as a consequence of the degradation of the amorphous regions and mostly to those of starch. These degraded fractions could crystallize in a greater extent, leading to a wider and more complex l distribution.

The crystallization of the degraded materials always showed the same pattern, with two peaks around 115 and 140°C (Fig. 3). The low-temperature peak was associated with the crystallization of PP and EVOH, and the high-temperature peak, which did not appear in the nondegraded material, was related to the crystallization of some degraded starch fractions.

On the other hand, the FTIR spectrum of the degraded materials did not show any carbonyl waveband. This result indicates that the PP matrix was practically unaffected by the degradation process.

Because the degradation process affected the crystallinity of the samples, the isothermal crystallization kinetics were studied for the nondegraded blend and for the blend subjected to degradation for 6 months. These crystallization processes were compared with the crystallization behavior of pure PP. Moreover, the crystallization of the blend at different degradation times was compared at a fixed temperature of 136°C.

The crystallization kinetics were analyzed by means of the Avrami equation:¹³

$$X(t) = 1 - \exp(-Kt^n) \quad (2)$$

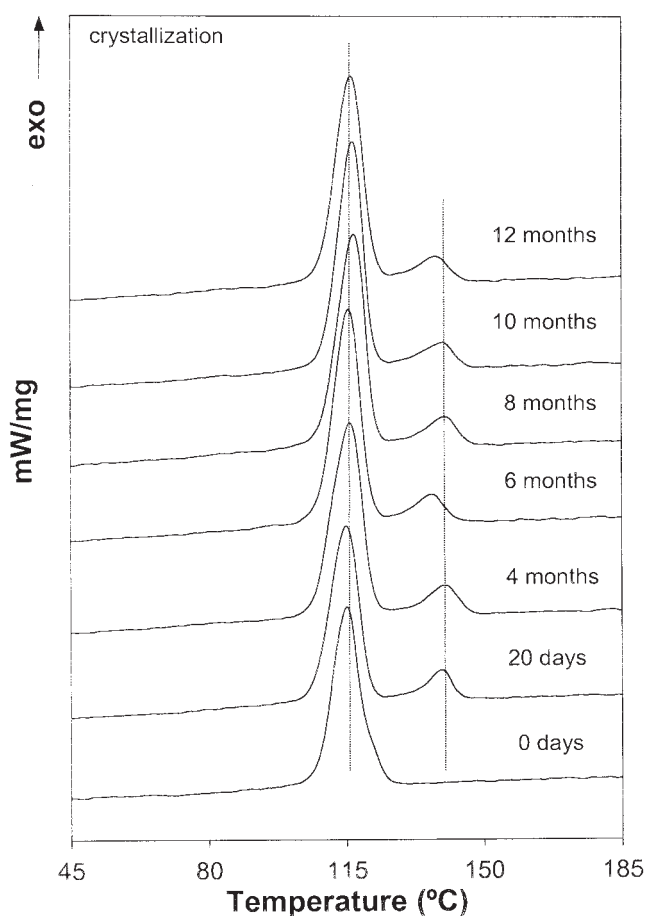


Figure 3 Crystallization of the PP/Mater-Bi blend as a function of the exposure time in soil.

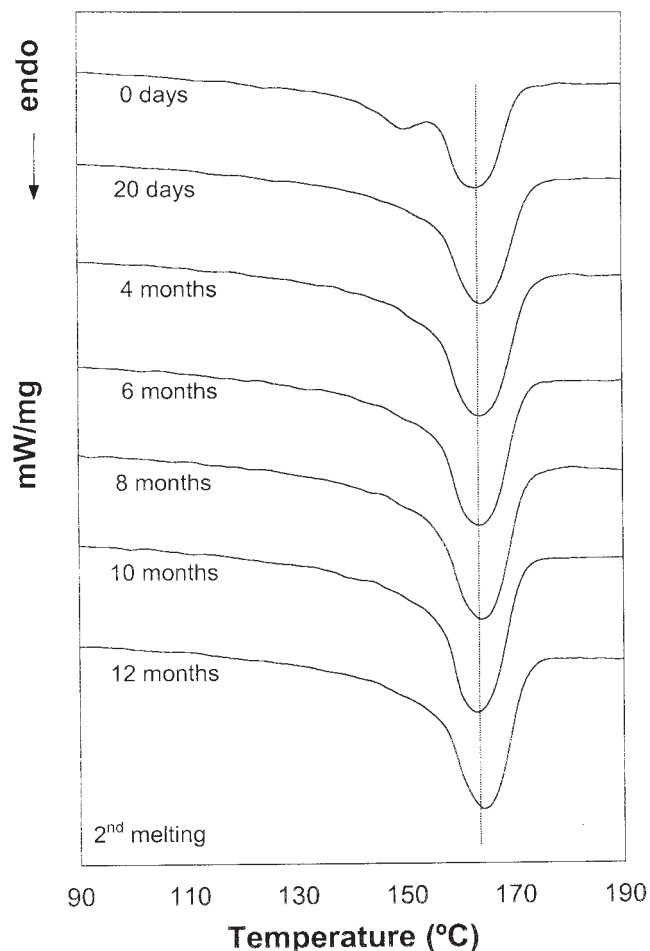


Figure 4 Second melting of the PP/Mater-Bi blend as a function of the exposure time in soil.

$$\ln[-\ln[1 - X(t)]] = n \ln(t) + \ln K \quad (3)$$

where $\chi(t)$ is the crystallized fraction or relative crystallization degree, t is the time, n is the Avrami exponent, and K is the isothermal crystallization constant. For each T_c , the linear plot of $\ln\{-\ln[1 - \chi(t)]\}$ versus $\ln t$ allowed the determination of n and $\ln K$ from the slope and the intercept, respectively.

$\chi(t)$ was calculated with the following equation:

$$X(t) = \frac{\Delta H_t}{\Delta H_{\text{iso}}} \quad (4)$$

where ΔH_t is the crystallization heat released until time t and ΔH_{iso} is the total isothermal crystallization heat. Both ΔH_t and ΔH_{iso} were obtained by the integration of the calorimetric signal until time t and until the end of the exothermic peak, respectively.

The crystallization half-time ($t_{1/2}$), defined as the time when $\chi(t)$ is 50%, was calculated from the Avrami equation [eq. (2)] as

$$t_{1/2} = \left(\frac{\ln 2}{K}\right)^{1/n} \quad (5)$$

The crystallization rate ($\tau_{1/2}$) was defined as the reciprocal of $t_{1/2}$:

$$\tau_{1/2} = \frac{1}{t_{1/2}} \quad (6)$$

TABLE II
Calorimetric Parameters of the PP/Mater-Bi Blend as a Function of the Exposure Time in Soil

Process	Exposure time	T_m (°C)		Δh_m (J/g)	χ (%)	I_{max} (Å)
		Main peak	Secondary peak			
First melting	—	167.3	134.6	99	52.8	203
	20 days	168.1	141.6	96	51.1	213
	4 months	172.9	151.5	105	55.9	305
	6 months	168.1	148.7	103	54.9	213
	8 months	168.1	151.3	98	52.2	213
	10 months	168.2	153.7	100	53.3	214
	12 months	167.4	155.2	103	54.4	204
Crystallization	—	115.6	—	64	34.1	—
	20 days	114.7	149.7	75	39.9	—
	4 months	115.7	140.5	85	45.3	—
	6 months	115.9	137.3	84	44.7	—
	8 months	117.5	140.6	88	46.9	—
	10 months	116.7	139.7	89	47.4	—
Second melting	12 months	116.6	138.0	87	46.3	—
	—	163.3	150.2	70	37.3	163
	20 days	164.0	—	78	41.5	169
	4 months	163.9	—	89	42.4	168
	6 months	163.8	—	88	46.9	167
	8 months	163.8	—	93	49.5	167
	10 months	163.0	—	94	50.1	161
	12 months	164.7	—	88	46.9	175

TABLE III
Avrami Kinetic Parameters Calculated from the Isothermal Crystallization Measurements at Different Temperatures

Sample	T_c (°C)	K (min ⁻ⁿ)	n	t_{12} (min)	$t_{1/2,exp}$ (min)	$\tau_{1/2}$ (min ⁻¹)
PP	136	1.81×10^{-3}	3.13	6.7	6.6	0.1493
	138	3.40×10^{-4}	3.24	10.5	10.4	0.0954
	140	8.20×10^{-5}	3.25	16.2	16.1	0.0619
	142	1.73×10^{-5}	3.24	26.5	25.8	0.0378
	144	5.54×10^{-6}	3.20	39.1	39.2	0.0256
PP/Mater-Bi	136	3.95×10^{-5}	2.76	34.7	32.3	0.0289
	138	1.32×10^{-5}	2.76	50.9	50.4	0.0196
	140	4.86×10^{-6}	2.68	83.2	85.2	0.0120
	142	1.08×10^{-6}	2.66	152.8	127.2	0.0065
	144	5.15×10^{-7}	2.62	220.7	220.2	0.0045
PP/Mater-Bi after 6 months in soil	136	1.52×10^{-4}	2.40	33.5	33.8	0.0299
	138	5.64×10^{-5}	2.40	50.2	50.9	0.0199
	140	7.78×10^{-5}	2.55	87.0	83.6	0.0115
	142	3.04×10^{-6}	2.55	126.8	152.7	0.0079
	144	3.62×10^{-7}	2.72	204.7	220.2	0.0049

$t_{1/2,exp}$, the experimental value of $t_{1/2}$.

To verify the calculated kinetic parameters (n and K), the experimental value of $t_{1/2}$ was compared with the value obtained from eq. (5).

K was evaluated from the Arrhenius equation:

$$\frac{\ln K}{n} = \ln k_0 - \frac{\Delta E}{RT_c} \quad (7)$$

where k_0 is the preexponential factor, ΔE is the activation energy, and R is the universal gas constant. The linear plot of $\ln K/n$ versus $1/T_c$ allowed us to deter-

mine ΔE and $\ln k_0$ from the slope and the intercept, respectively.

Table III shows the Avrami kinetic parameters obtained from the isothermal crystallization of pure PP and the PP/Mater-Bi blend before and after degradation. Figure 5 shows, as an example, the calorimetric curves of the crystallization of PP at different temperatures. In all cases, $\tau_{1/2}$ increased as the temperature decreased. This result can be explained by the fact that crystallizations from the melt exhibited a dependence on the temperature, which is characteristic of nucle-

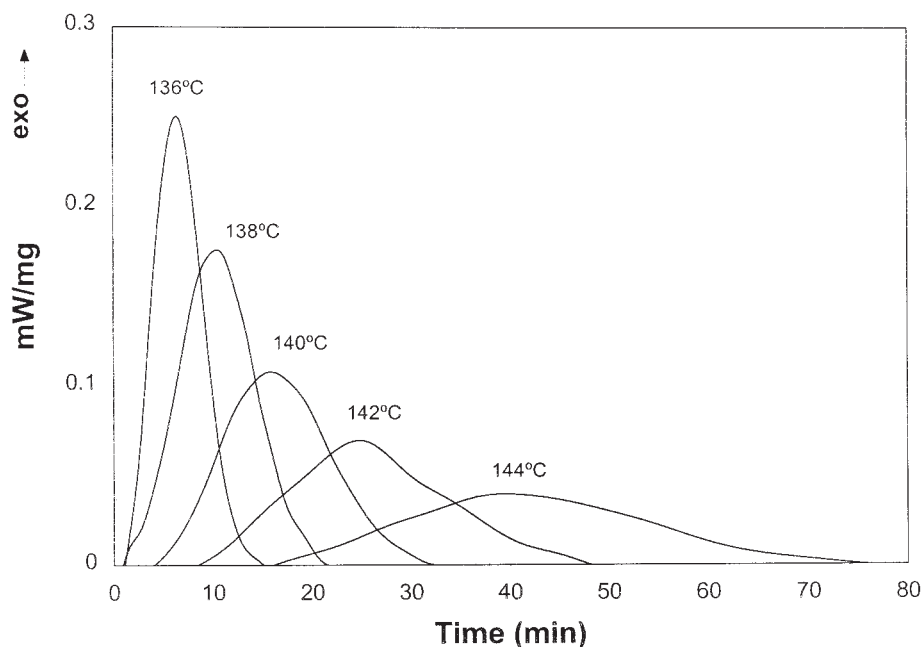


Figure 5 Isothermal crystallizations at different temperatures of pure PP.

TABLE IV
 ΔE 's and Frequency Factors Calculated from the Isothermal Crystallization Measurements

	PP	PP/Mater-Bi	PP/Mater-Bi after 6 months in soil
ΔE (kJ/mol)	315.7	343.5	319.6
k_0 (min ⁻¹)	6.50×10^{-42}	5.69×10^{-46}	4.07×10^{-43}

ation-controlled crystallizations. Also, the PP/Mater-Bi blend crystallized more slowly than pure PP, due to the interaction of EVOH and starch onto the PP matrix.

The n values found in the literature show disparate values but are usually between 1.8 and 4 for PP. In most cases, these differences can be explained from the different thermal treatments of the materials.¹⁴ However, in this case, where the thermal treatment was fixed and was the same for all of the samples under study, changes in the values of n must have evidenced differences in the microstructure. The value of n was sensitive both to the blending process and to the degradation process. Pure PP showed a mean value of $n = 3.2$, whereas the mean value for the blend was $n = 2.7$. This latter decreased to 2.5 after the 6-month degradation. A value of $n = 4$ suggests an homogeneous nucleation and tridimensional crystalline growth, whereas values of $n = 3$ and $n = 2$ can be associated to a tridimensional and bidimensional growth, respectively, with heterogeneous nucleations.¹⁵ We conclude, then, that both the blending and degradation processes led to changes in the crystallization type of the samples.

The ΔE 's and the k_0 's of these crystallizations are shown in Table IV. In general, all of the samples exhibited similar kinetic parameters, although the 6-month degraded sample showed kinetic parameters apparently closer to those of pure PP than to those of the nondegraded sample. This effect was just fictitious because the degraded and nondegraded blends displayed similar $\tau_{1/2}$'s (Table III). This could have possibly been due to the fact that the differences between the k_0 values were compensated by the differences between the ΔE 's (compensation effect).

Figure 6 compares the calorimetric curves of the crystallizations at 136°C of the PP/Mater-Bi blend after different degradation times. Table V shows the kinetic parameters related to these crystallizations. In general, although slight fluctuations were observed, for longer degradation times, the crystallization process showed higher $\tau_{1/2}$'s and lower crystallization times. On the other hand, the n decreased until the 4th degradation month and afterward remained constant; this evolution was in agreement with that underwent by the calorimetric parameters with the degradation time. Therefore, $\tau_{1/2}$ and n seemed to be indicative parameters of the degree of degradation.

On the other hand, the comparison between the experimental values of $t_{1/2}$ and those calculated with eq. (5) (Tables III and V) evidenced that the methodology we employed was proper.

CONCLUSIONS

From the obtained results, we can state that the blends of PP with Mater-Bi AF05H subjected to biodegradation in soil undergo certain morphological changes,

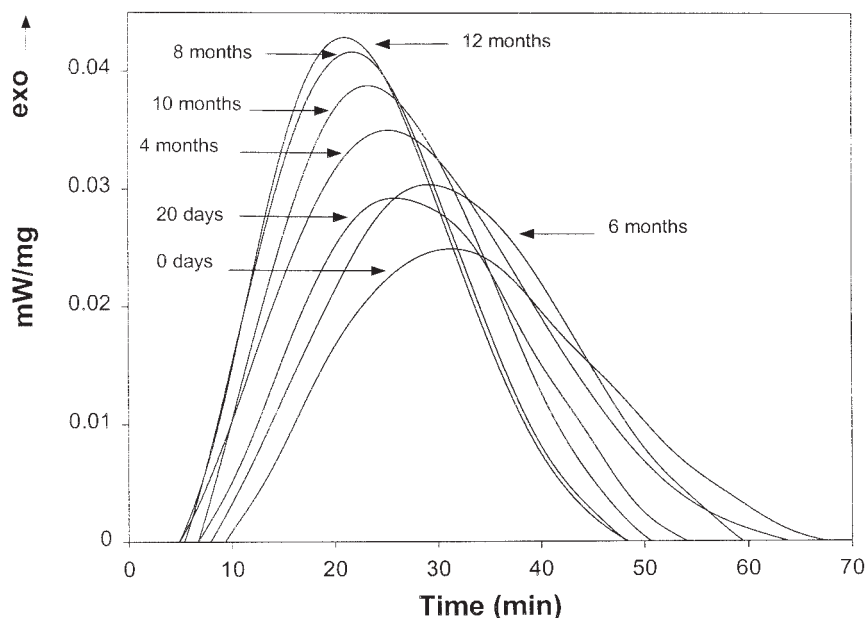


Figure 6 Crystallizations at 136°C of the PP/Mater-Bi blend after different exposure times in soil.

TABLE V
Avrami Kinetic Parameters Calculated from the Crystallization Measurements at 136°C
for the PP Mater-Bi Blend Degraded in Soil for Different Times

Degradation time	K (min^{-n})	n	$t_{1/2}$ (min)	$t_{1/2 \cdot \text{exp}}$ (min)	$\tau_{1/2}$ (min^{-1})
—	3.38×10^{-5}	2.80	34.8	33.8	0.0288
20 days	2.24×10^{-4}	2.38	29.4	28.8	0.0340
4 months	4.12×10^{-4}	2.17	30.5	29.0	0.0328
6 months	1.64×10^{-4}	2.40	32.7	31.8	0.0306
8 months	3.09×10^{-4}	2.39	25.2	24.6	0.0397
10 months	2.56×10^{-4}	2.38	27.8	27.3	0.0360
12 months	3.66×10^{-4}	2.39	23.4	23.3	0.0427

$t_{1/2 \text{ exp}}$, the experimental value of $t_{1/2}$.

proved by the changes on crystallinity and the l distribution of PP.

With an increase of crystallinity considered a sign of degradation, we found that the blends underwent a certain degradation until the 4th month, and then their degradation seemed to slow down.

The calorimetric results suggest that the degradation process started in the amorphous regions of the starch and did not significantly affect the PP matrix. This could have been due to the heterogeneous character of the PP/Mater-Bi blend so that the degradation of the amorphous regions of the starch was not enough to induce the degradation of the other components of the sample.

The Avrami equation and the isothermal crystallization analysis allowed a proper description of the crystallization kinetics of pure PP and both the degraded and nondegraded blends.

The analysis of the crystallization kinetics showed that $\tau_{1/2}$ and n reflected the effect of both the blending process and degradation on the crystallization of these materials, and thus, both of them can be used as indicative parameters of these processes.

References

- Griffin, G. J. L. Chemistry and Technology of Biodegradable Polymers; Blackie: Glasgow, 1994.
- Bastioli, C. Polym Degrad Stab 1998, 59, 263.
- Schnabel, W. Polymer Degradation: Principles and Practical Applications; Hanser: Munich, 1992.
- Albertsson, A. C.; Andersson, S. V.; Karlsson, S. Prog Polym Sci 1987, 18, 73.
- Albertsson, A. C.; Karlsson, S. Prog Polym Sci 1990, 15, 177.
- Contat-Rodrigo, L.; Ribes-Greus, A.; Diaz-Calleja, R. J Appl Polym Sci 2001, 82, 2174.
- Testing of Plastics. Influence of Fungi and Bacteria. Visual Evaluation: Change in Mass and Physical Properties; DIN 53739; Beuth Verlag GmbH: Berlin, 1984.
- Goheen, S. M.; Wool, R. P. J Appl Polym Sci 1991, 42, 2691.
- Sousa, R. A.; Kalay, G.; Reis, R. L.; Cunha, A. M.; Bevis, M. J. J Appl Polym Sci 2000, 77, 1303.
- Van Krevelen, D. W. Properties of Polymers, 3rd ed.; Elsevier: Amsterdam, 1994.
- Wlochowicz, A.; Eder, M. Polym 1984, 25, 1268.
- Hawkins, W. Polymer Degradation and Stabilization; Springer-Verlag: Berlin, 1984.
- Avrami, M. J. Chem Phys 1939, 7, 1103.
- Lu, H.; Qiao, J.; Yang, Y. Polym Int 2002, 51, 1304.
- Sesták, J. Thermophysical Properties of Solids: Comprehensive Analytical Chemistry. Vol. XII. Thermal Analysis; Svehla, G., Ed.; Elsevier: Amsterdam, 1984; p 212.